CHEMICAL ENGINEERING TRANSACTIONS
VOL. 106, 2023
A publication of AIDIC
The Italian Association of Chemical Engineering
Online at www.cetjournal.it
Guest Editors: Jeng Shiun Lim, Nor Alafiza Yunus, Peck Loo Kiew, Hon Huin Chin

ISBN 979-12-81206-05-2; **ISSN** 2283-9216
DOI: 10.3303/CET23106184

Effect of Gas Compositions on Binary CO_2-N_2 Adsorption of Pomelo Peel-based Activated Carbon

Nawal A. Ghafar[a], Nurfatehah Wahyuny Che Jusoh[a,b,*], Nor Ruwaida Jamian[a]

[a]Department of Chemical and Environmental Engineering (ChEE), Malaysia-Japan International Institute of Technology (MJIIT), Universiti Teknologi Malaysia Kuala Lumpur, Malaysia
[b]Center of Hydrogen Energy, Institute of Future Energy, Universiti Teknologi Malaysia Kuala Lumpur, Malaysia
nurfatehah@utm.my

Activated carbon derived from biomass sources is one of the most promising adsorbents for carbon dioxide (CO_2) capture because it is inexpensive, effective, and environmentally friendly. The increment of CO_2 in the atmosphere is the root cause of numerous climate change-centric environmental problems, in which one of the major CO_2 emission sources is known to be the fossil-fuelled power plant. The most mature CO_2 capture system (post-combustion capture) of fossil-fuelled power plants involves capturing CO_2 from flue gas at low CO_2 composition (5–15 wt%), with the remaining gas composed mainly of nitrogen (N_2). Hence, this study investigated the effect of the CO_2 and N_2 gas compositions on the binary CO_2-N_2 adsorption performances of the activated carbon derived from pomelo peel (PP). Moreover, the comparison of the adsorption performance between pomelo peel-based activated carbon (PPAC) and commercial activated carbon (COMM-AC) was also evaluated. Besides that, PP and PPAC were also characterized through Fourier Transform Infrared (FTIR), X-Ray Diffraction (XRD), and Brunauer-Emmett-Teller (BET) analysis. The results demonstrated that PPAC has a low graphitization degree and possess a microporous-mesoporous structure, with the pores mainly composed of micropores. The attained results on the effect of the gas compositions showed that higher CO_2 gas composition leads to a higher binary CO_2-N_2 uptake, indicating that PPAC is more selective towards CO_2 than N_2. By comparing the adsorption performance of PPAC and COMM-AC, it was inferred that COMM-AC is a superior adsorbent at a higher pressure and CO_2 composition condition. In contrast, PPAC was found to be a better adsorbent at a lower pressure and CO_2 composition condition. These results signified that PPAC is a potential adsorbent for CO_2 gas, especially in post-combustion flue gas conditions.

1. Introduction

Climate change and global warming are alarming environmental issues predominantly caused by an excessive concentration of greenhouse gases in the atmosphere, with majority comes from CO_2 gas. It is reported that CO_2 makes up approximately 76 % of the greenhouse gases emitted into the atmosphere (Fletcher and Smith, 2020). Therefore, it is necessary to actively implement the appropriate strategy to reduce the CO_2 in the atmosphere. Carbon Capture and Storage (CCS) is a CO_2 reduction strategy centred on capturing CO_2 from primary CO_2 producers and storing it. One of the main CO_2 producers is fossil-fuelled power plants (contributing around 86 % of the overall anthropogenic CO_2 emission) (Dodevski et al., 2020). Three types of CO_2 capture systems can be integrated into fossil-fuelled power plants: pre-combustion capture, oxyfuel combustion capture, and post-combustion capture. Among these CO_2 capture systems, post-combustion capture is considered the most mature and flexible due to its retrofitting readiness to the existing system in the power plant. This capture system involves capturing CO_2 after the combustion process of the fossil fuel, in which the flue gas from the combustion process is typically a diluted CO_2 stream (5–15 wt% CO_2), with N_2 being the main constituent of the remaining gas. The CO_2 composition of the post-combustion flue gas varies with the type of fossil fuel used – natural gas (~5 wt%) and coal (~10–15 wt%) (Amann and Bouallou, 2009). Therefore, CO_2 capture must be carried out at this gas composition range to simulate the typical post-combustion capture conditions in fossil-fuelled power plants.

Paper Received: 05 March 2023; Revised: 25 July 2023; Accepted: 11 October 2023
Please cite this article as: Ghafar N.A., Jusoh N.W.C., Jamian N.R., 2023, Effect of Gas Compositions on Binary CO2-N2 Adsorption of Pomelo Peel-based Activated Carbon, Chemical Engineering Transactions, 106, 1099-1104 DOI:10.3303/CET23106184

The most common CO_2 capture method deployed in the industry nowadays is amine-based liquid absorption. This conventional method, however, possesses a few drawbacks that include solvent degradation and being expensive due to the high regeneration cost. Adsorption is a promising alternative to this conventional method since it is regarded as an effective and inexpensive method (due to its low regeneration cost). One of the most effective adsorbents that can be utilized for the CO_2 adsorption process is activated carbon - a carbon-rich material with an abundance of pores. Since the available commercial activated carbon is considered an expensive adsorbent, there have been numerous studies on utilizing various low-cost precursor materials for the synthesis of activated carbon, particularly biowaste materials. Pomelo (*Citrus grandis osbeck*) fruit is known as the largest fruit in the citrus family, and it can be found abundantly in China and Southeast Asia (Tocmo et al., 2020). Due to it being large in size, its peel is considered a hefty biowaste since it can generally account for up to half of the fruit's weight. Its utilization as an activated carbon precursor was exhibited in a few previous studies for application as supercapacitor material (Fu et al., 2018). Moreover, a recent work studied the pomelo peel-based activated carbon (PPAC) as an adsorbent for Pb (II) (Dinh et al., 2022). Although there have been several studies on using PPAC, there is no reported study regarding its use as an adsorbent for CO_2 adsorption. In this study, the PPAC was used as an adsorbent to study the effects of the different gas compositions on its binary CO_2-N_2 adsorption performance. Moreover, the characterizations of the PPAC were carried out to evaluate its physicochemical properties as an adsorbent. In addition, the adsorption performance of the PPAC was also compared with the commercial activated carbon (COMM-AC).

2. Materials and methods

The synthesis of the PPAC was carried out through chemical activation, in which the activation agent used is potassium hydroxide (KOH). The type of characterizations that were conducted on PP and PPAC are Fourier Transform Infrared (FTIR), X-Ray Diffraction (XRD) and Brunauer-Emmett-Teller (BET) analysis. The gas adsorption measurement was carried out using gravimetric adsorption equipment.

2.1 Materials

PP were obtained from M&H fruit store in Shah Alam, Selangor, Malaysia. The analytical grade of potassium hydroxide (KOH) was acquired from R&M Chemicals, Malaysia. The COMM-AC powder (produced from coconut shells) was acquired from Chemiz, Malaysia. The carbon dioxide, nitrogen, and argon gas with a purity of 99.999 % were purchased from Alpha Gas Solutions, Malaysia.

2.2 Synthesis of activated carbon from pomelo peel

PP were washed repeatedly with distilled water and cut into small dice. It was dried inside an oven for 24 h to remove the moisture and further ground into powders. After that, the dried PP were carbonized inside a tubular furnace with a continuous argon gas flow for 2 h at 600 ºC. 5 g of the carbonized PP was mixed with 15 g of KOH in a 100 mL solution, and the mixture was stirred at 80 ºC for 6 h. It was then activated inside a furnace with a continuous argon gas flow at 700 ºC for 1.5 h. This is followed by repeated hydrochloric acid (HCl) and distilled water washing until the filtrate pH was 7. Lastly, it was dried inside an oven for 24 h.

2.3 Characterization

FTIR analysis was carried out on PP and PPAC to identify the functional groups on their respective surface. Shimadzu IR-Tracer 100 with potassium bromide (KBr) pellet method was used for the FTIR analysis, where the FTIR spectra recorded are in the wavelength region of 500–4,000 cm^{-1}. The crystallinities of PP and PPAC were examined using PanAnalytical X-Ray Diffractometer (Model: Empyrian Series 2), with CuKα (λ = 1.54 Å) radiation at 40 mA and 45 kV. The XRD diffractograms recorded are in the range of $5° < 2\theta < 90°$. The pore characteristics (surface area, pore volume, pore size distribution) of PP and PPAC were evaluated from the BET analysis, in which the adsorption-desorption of N_2 gas at -196 ºC (77K) was carried out using Micrometritics ASAP 2020.

2.4 Gas Adsorption measurement

The gas adsorption measurement of PPAC was performed via the gravimetric adsorption method using Rubotherm isoSORP Gravimetric Analyzer. This equipment depends on a magnetic suspension balance (MSB) to accurately measure the mass change of the adsorbent before and after the adsorption process. Figure 1 shows the illustration of the MSB comprising of several affecting forces in the system (buoyancy force, gravitational force, and force from the gas adsorption). The initial step of using this equipment is the pretreatment step, whereby the sample was initially degassed in a vacuum condition and high temperature to eliminate moisture and adsorbed gases from the samples. This is followed by the buoyancy measurement of the sample using helium gas (He) to precisely determine its mass and volume. Finally, the gas adsorption process was

carried out at an adsorption temperature of 25ºC and pressures from 0 to 10 bar. For each pressure reading, the equilibrium adsorption capacity at equilibrium condition is automatically measured by the equipment. The mass of the adsorbed gas and the adsorption capacity of the adsorbent are calculated from Eq (1) and Eq (2). Eq (1) is derived from the balance of affecting forces in MSB, as observed in Figure 1. The gas adsorption measurement was performed at gas compositions of 100 % CO_2, 100 % N_2, 5 %CO_2-95 % N_2, 10 % CO_2-90 % N_2, and 15% CO_2-85 % N_2. For comparison purposes, the gas adsorption measurement was also conducted for COMM-AC at the same adsorption conditions as PPAC.

$$Mass\ of\ adsorbed\ gas, m_A\ (g) = m_{SB} - m_{SH} - m_s + (V_{SH} + V_S + V_A)\rho_g \quad (1)$$

$$Adsorption\ capacity\ (mg/g) = \frac{m_A}{m_S}\ x\ 1000 \quad (2)$$

Where m_{SB} (g) is the weight reading from the balance, m_{SH} (g) is the mass of sample holder, m_S (g) is the mass of sample, V_{SH} (cm^3) is the volume of the sample holder, V_S (cm^3) is the volume of the sample, V_A(cm^3) is the volume of the adsorbed gas, and p_g (g/cm^3) is the density of the gas.

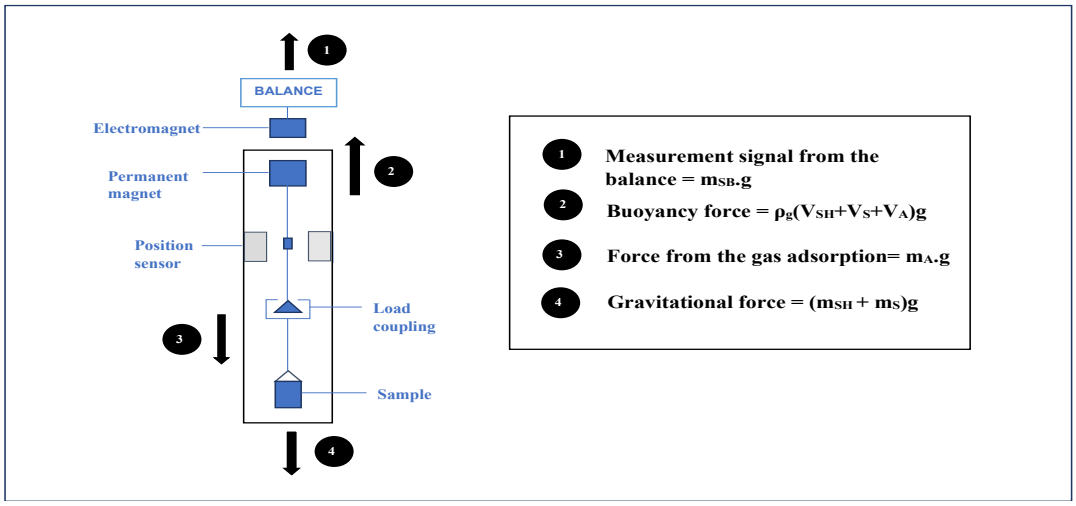

Figure 1: Schematics of the Rubotherm magnetic suspension balance

3. Results and discussion

3.1 Characterization of PP and PPAC

The surface functional groups of PP and PPAC are identified from the FTIR Spectra in Figure 2(a). PP exhibits a strong and broad band at 3,430 cm^{-1} that signifies the presence of O-H stretching on the cellulose and lignin structure of PP. The peak at 2,912 cm^{-1} denotes the existence of C-H stretching in the methyl group. The peaks at 1,746 cm^{-1} and 1,633 cm^{-1} are attributed to C=O stretching in carboxyl and lactone (Chen et al., 2014). The absorption band at 1,439cm^{-1} indicates the presence of alkane C-H stretching, whereas the peaks at 1,308 cm^{-1}, 1,248 cm^{-1},1,101 cm^{-1}, and 1,013cm^{-1} are ascribed to C-O stretching from ester, ether, alcohol and carboxylic acid groups in the cellulose and hemicellulose structure (Singh et al., 2017).

From the comparison of the FTIR spectrum of PPAC and PP, it is observed that multiple peaks (2,912 cm^{-1}, 1,633cm^{-1}, 1,439cm^{-1}, 1,308cm^{-1}, 1,248cm^{-1}) had disappeared in the PPAC spectrum, which denotes that multiple functional groups were volatilized during the carbonization and KOH activation process of PP. An absorption band of O-H stretching (3,430cm^{-1}) and C=O stretching (1,746cm^{-1}) are present in the PPAC spectrum, although at a much lower intensity than that of PP. This suggests a possible reduction in the respective functional groups due to their partial degradation from the carbonization and activation process of PP. The emergence of a new peak at 1,520 cm^{-1} indicates the presence of C=C stretching in the carbon structure, which is possibly attributed to the intermolecular dehydration during the activation process (Jawad et al., 2018). Moreover, two strong peaks are also observed at 1,121cm^{-1} and 959cm^{-1}, which correspond to the stretching vibration of C-O on PPAC

Figure 2(b) shows the XRD diffractograms of PP and PPAC. From Figure 1(b), PP exhibited crystalline and amorphous phases, whereby the amorphous phase is ascribed to its hemicellulose and lignin structure. The three diffraction peaks of PP at 16°, 22°, and 35° are identified as (110), (200), and (400) crystalline cellulose I

peaks, in which the crystalline region of the cellulose structure is attributed to both van der Waals forces of the glucose molecules and hydrogen bonding of the cellulose chains (He et al., 2022). The diffraction spectrum of PPAC contains two broad peaks at 23° and 43° that are assigned to the (002) and (100) graphitic carbon plane. The amorphous halo of these peaks indicates that PPAC has a low degree of graphitization and consists of a few graphite crystals (Fu et al., 2018). Its low degree of graphitization and crystallinity generally mean that PPAC is probably composed of a highly porous structure with abundant structural defects. This can result to a high availability of energetically favoured adsorption sites for the CO_2 gas molecules (Yang et al., 2022). The existence of an additional peak at ~29° is probably due to the residue of potassium chloride (KCl) that was left from the neutralization reaction of HCl and KOH during the washing process, as observed in activated carbon preparation from the tea seed shell (Quan et al., 2020).

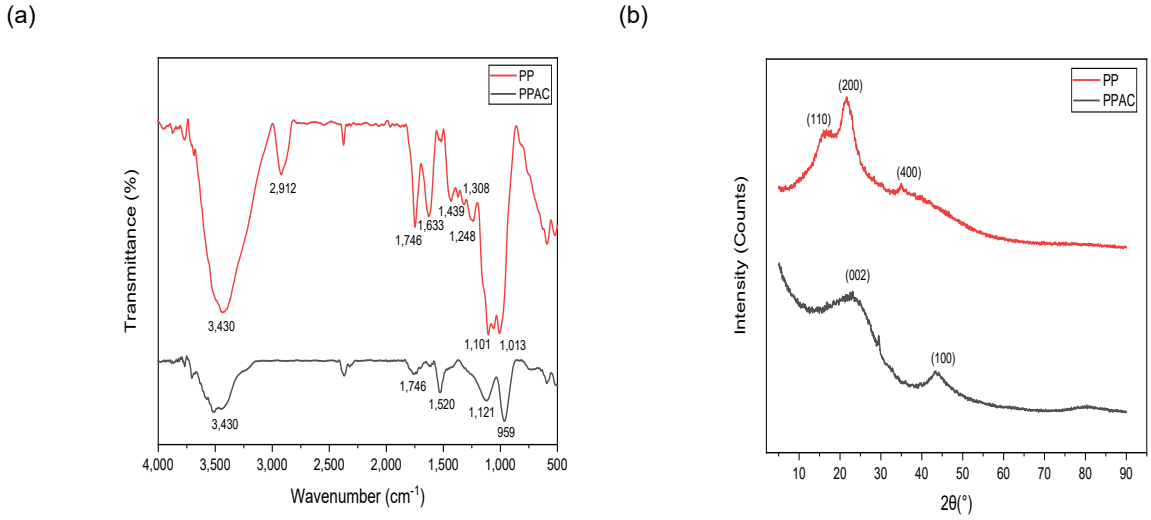

Figure 2: (a) FTIR Spectra and (b) XRD Diffractograms of PP and PPAC

The textural properties of PP and PPAC are summarized in Table 1. From Table 1, it is shown that PPAC has a significantly higher porosity than pristine PP, as evident from its comparison of the specific surface area value and total pore volume. This comparison indicates that abundant pores were successfully generated during the carbonization and KOH activation process of PP. From the value of the micropore and mesopore volume, it is surmised that the pore structure of PPAC is a microporous-mesoporous structure, with the pores composed mainly of micropores (69 % of micropores). The average pore diameter of the microporous-mesoporous structure of PPAC is around 2.859 nm. The presence of micropores is beneficial to the CO_2 adsorption process since micropores can retain the CO_2 molecules from the overlapping interactions of the pore wall (Chiang et al., 2019). Besides that, the presence of mesopores is also known to be beneficial to gas adsorption as it can speed up the diffusion of the gas into the pores.

Table 1: Textural properties of PP, PPAC, and COMM-AC

Sample	BET Specific Surface Area (m^2/g)	Total Pore Volume (cm^3/g)	Micropore Volume (cm^3/g)	Mesopore Volume (cm^3/g)	Average Pore Diameter (nm)
PP	1.516	0.002	-	-	6.706
PPAC	455.537	0.235	0.161	0.074	2.859
COMM-AC	1150.0	-	-	-	-

3.2 Effect of gas compositions on CO_2-N_2 adsorption of PPAC

The effect of the CO_2 and N_2 gas compositions on the adsorption performance of the PPAC adsorbent is depicted in Figure 3(a). The varied gas compositions are 5 % CO_2-95 % N_2, 10 % CO_2-95 % N_2, and 15 % CO_2-85 % N_2, which mimic the typical post-combustion flue gas composition in fossil-fuelled power plants. The adsorption performances of pure CO_2 and N_2 were also included in this study. Based on Figure 3(a), it is exhibited that the adsorption capacity of the CO_2-N_2 gas mixture for the entire pressure range increased with the CO_2 gas compositions. For instance, at a total pressure of 1 bar, the highest adsorption capacity value of

55.7 mg/g was attained for 15 % CO_2 gas composition, followed by 49.1 mg/g and 38.3 mg/g for 10 % and 5 % CO_2 gas composition. In addition, it is also shown that the pure CO_2 uptake is significantly higher than the pure N_2 uptake. These results signified that PPAC selectively adsorbed CO_2 from the gas mixture compared to N_2. This is probably due to these gases' respective properties, which include their polarizability and quadrupole moment. These properties of the adsorbate gas are imperative in evaluating the strength of the adsorbate-adsorbent interaction; higher polarizability and quadrupole moment of the adsorbate gas equates to stronger electrostatic interaction between the adsorbate and adsorbent. Since the CO_2 molecule possesses 1.5-times higher polarizability (CO_2: 26.5 x10^{-25} cm^3 vs. N_2:17.6x10^{-25} cm^3) and 3-times higher quadrupole moment (CO_2: 4.3x10^{26} esu cm^2 vs N_2: 1.52x10^{26} esu cm^2) than N_2 molecule, a stronger interaction between CO_2 molecule and PPAC is expected (Mulgundmath et al., 2012). Thus, this shows that higher CO_2 composition in CO_2-N_2 gas mixture leads to a stronger interaction between the CO_2 molecules and the surface of PPAC, which consequently results in a higher adsorption capacity of the adsorbent.

3.3 Comparison of PPAC and COMM-AC

The comparison of the adsorption performance between PPAC and COMM-AC from Chemiz is illustrated in Figure 3(b). From the comparison in Figure 3(b), the first acquired observation is that COMM-AC showcased better adsorption performance than PPAC in a higher pressure and CO_2 composition region. At the highest pressure of 10 bar, the pure CO_2 uptake of COMM-AC was measured at a value of 272.3 mg/g, which is higher than the CO_2 uptake of PPAC (214.3 mg/g). The reason for this attained result is probably due to the significantly higher surface area of COMM-AC (1150 m^2/g) compared to PPAC (455.5 m^2/g). On the other hand, in a lower pressure and CO_2 composition region, it is shown that PPAC has a better adsorption performance than COMM-AC. For instance, at 1 bar and 5 % CO_2 composition, a higher adsorption capacity value of 38.3 mg/g is recorded for PPAC, as opposed to 31.6 mg/g for COMM-AC. The pure CO_2 uptake at 1 bar is also higher for PPAC (128.7 mg/g) than COMM-AC (121.2 mg/g). These findings are probably attributed to the pore size distribution of the adsorbent, suggesting that PPAC probably has more abundant smaller-sized micropores than COMM-AC. The overlapping of the attractive fields between the micropore walls leads to an enhancement of the physisorption of the gas. These results are consistent with previous studies of activated carbon derived from cashew nutshell (Rao et al., 2018) and lotus stalk (Garg and Das, 2019), which attributed their high CO_2 adsorption capacity to the microporosity of the adsorbent.

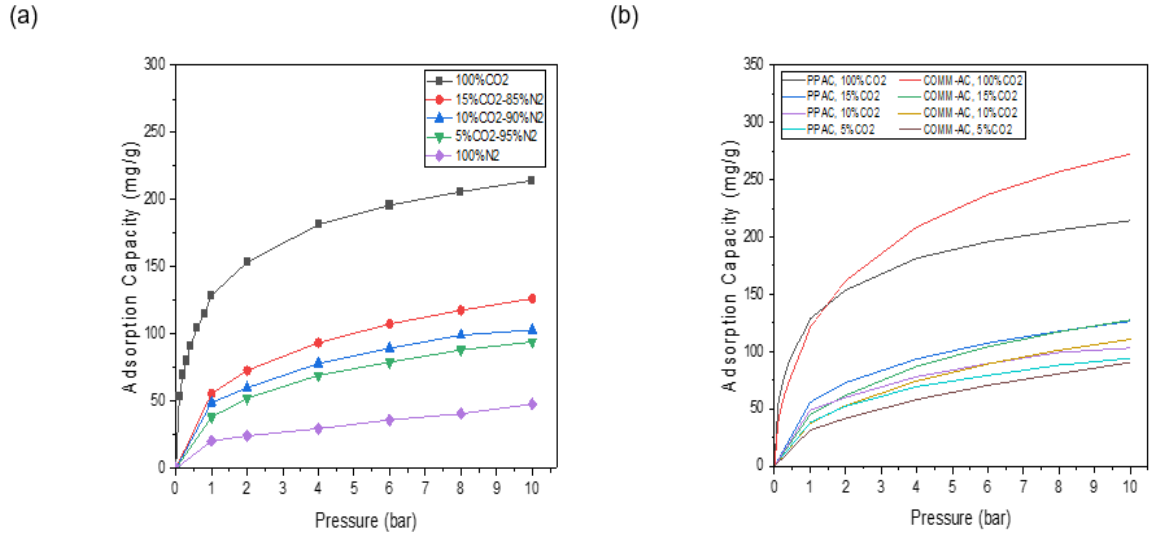

Figure 3: (a) Effect of gas compositions on CO_2-N_2 adsorption of PPAC and (b) Adsorption isotherm comparison of PPAC and COMM-AC

4. Conclusions

The aim of this study is to investigate the effect of gas compositions on the binary CO_2-N_2 adsorption performance of PPAC. The adsorption performance of PPAC showed that an increase in CO_2 gas composition of CO_2-N_2 mixture from 5 to 15% resulted in a higher adsorption performance of the adsorbent (38.3 to 55.7 mg/g at ambient conditions), indicating that PPAC strongly adsorbed CO_2 in comparison to N_2. This is possibly attributed the higher innate properties of CO_2 (polarizability and quadrupole moment). By comparing the gas adsorption performance of PPAC with COMM-AC at similar gas compositions range, it is showed that COMM-

AC is a superior adsorbent in a higher pressure and CO_2 composition region due to the higher surface area of the COMM-AC. At the highest pressure of 10 bar, COMM-AC achieved pure CO_2 uptake of 272.3 mg/g, as opposed to 214.3 mg/g for PPAC. On the other hand, PPAC is demonstrated as a better adsorbent in a lower pressure and CO_2 composition region, which yielded a value of 38.3 mg/g compared to 31.6 mg/g for COMM-AC at 5 % CO_2 composition and pressure of 1 bar. Based on these results, it is inferred that PPAC is a promising adsorbent for CO_2 adsorption at post-combustion flue gas conditions.

Acknowledgments

The authors are appreciative of the financial support provided by Ministry of Education (MOE) through Fundamental Research Grant Scheme (Ref:FRGS/1/2022/STG05/UTM/02/2 – Interaction of ZnO/g-C3N4 with Polypropylene Non-woven Fabric for Enhanced Continuous Flow Photodegradation of Cosmetic Industrial Wastewater) and Malaysia-Japan International Institute of Malaysia, Universiti Teknologi Malaysia.

References

Amann J.M.G., Bouallou C., 2009, CO_2 capture from power stations running with natural gas (NGCC) and pulverized coal (PC): Assessment of a new chemical solvent based on aqueous solutions of N-methyldiethanolamine + triethylene tetramine', Energy Procedia, 1(1), 909–916.

Chen L.C., Peng P.Y., Lin L.F., Yang T.C.K., Huang C.M., 2014, Facile preparation of nitrogen-doped activated carbon for carbon dioxide adsorption, Aerosol and Air Quality Research, 14(3), 916–927.

Chiang Y.C., Yeh C.Y., Weng C.H., 2019, Carbon dioxide adsorption on porous and functionalized activated carbon fibers, Applied Sciences, 9(10), 1977.

Dinh V., Nguyen D., Luu T., Nguyen Q., Thi T., Nguyen P., Dong T., Thi P., Thi N., Hue N., 2022, Adsorption of Pb (II) from aqueous solution by pomelo fruit peel-derived biochar, Materials Chemistry and Physics, 285, 126105.

Dodevski V., Janković B., Radović I., Stojmenović M., Čebela M., Nikolić Ž., Pagnacco M.C., Panić I., Stanković M., 2020, Characterization analysis of activated carbon derived from the carbonization process of plane tree (*Platanus orientalis*) seeds, Energy and Environment, 31(4), 583–612.

Fletcher W.D., Smith C.B., 2020, Reaching Net Zero, Elsevier, Amsterdam, Netherlands, 1–8.

Fu G., Li Q., Ye J., Han J.J., Wang J., Zhai L., Zhu Y., 2018, Hierarchical porous carbon with high nitrogen content derived from plant waste (pomelo peel) for supercapacitor, Journal of Materials Science: Materials in Electronics, 29(9), 7707–7717.

Garg S., Das P., 2019, Microporous carbon from cashew nutshell pyrolytic biochar and its potential application as CO_2 adsorbent, Biomass Conversion and Biorefinery, 10, 1043-1061.

He C., Li H., Hong J., Xiong H., Ni H., Zheng M., 2022, Characterization and functionality of cellulose from pomelo fruitlets by different extraction methods, Polymers, 14(3), 1–13.

Jawad A.H., Ngoh Y.S., Radzun K.A., 2018, Utilization of watermelon (*Citrullus lanatus*) rinds as a natural low-cost biosorbent for adsorption of methylene blue: Kinetic, equilibrium and thermodynamic studies, Journal of Taibah University for Science, 12(4), 371–381.

Mulgundmath V.P., Tezel F.H., Saatcioglu T., Golden T.C., 2012, Adsorption and separation of CO_2 /N_2 and CO_2/CH_4 by 13X zeolite, The Canadian Journal of Chemical Engineering, 90, 730–738.

Quan C., Jia X., Gao N., 2020, Nitrogen-doping activated biomass carbon from tea seed shell for CO_2 capture and supercapacitor, International Journal of Energy Research, 44(2),1218–1232.

Rao L., Yue L., Wang L., Wu Z., Ma C., An L., Hu X., 2018, Low-temperature and single-step synthesis of N-doped porous carbons with a high CO_2 adsorption performance by sodium amide activation, Energy and Fuels, 32(10), 10830-10837.

Singh G., Kim I.Y., Lakhi K.S., Srivastava P., Naidu R., Vinu A., 2017, Single step synthesis of activated bio-carbons with a high surface area and their excellent CO_2 adsorption capacity, Carbon, 116, 448–455.

Tocmo R., Pena-Fronteras J., Calumba K.F., Mendoza M., Johnson J.J., 2020, Valorization of pomelo (*Citrus grandis* Osbeck) peel: A review of current utilization, phytochemistry, bioactivities, and mechanisms of action, Comprehensive Reviews in Food Science and Food Safety, 19(4), 1969–2012.

Yang M., Cui C., Liu L., Dai L., Bai W., Zhai J., Jiang S., Wang W., Ren E., Cheng C., Guo R., 2022, Porous activated carbons derived from bamboo pulp black liquor for effective adsorption removal of tetracycline hydrochloride and Malachite Green from water, Water Science and Technology, 86(2), 244–260.